

Valve friction quantification and nonlinear process model identification

Rodrigo A. Romano* Claudio Garcia**

* Polytechnic School, University of São Paulo, São Paulo, Brazil
(Tel: +55 11-30911893, e-mail: rovite@gmail.com)

** Polytechnic School, University of São Paulo, São Paulo, Brazil
(Tel: +55 11-30915648, e-mail: clgarcia@lac.usp.br)

Abstract:

This paper extends existing methods that jointly estimate the process and friction model parameters, so that a nonlinear process model structure is considered. In addition, nonlinear optimization is applied to estimate the friction model parameters. The developed estimation algorithm is tested with data generated by a hybrid setup (composed of a real valve and a simulated pH neutralization process), in which the influences of the excitation signal magnitude and of the controller tuning on estimated models are investigated. The results demonstrate that the friction is accurately quantified, as well as “good” process models are estimated in several situations. In addition, the proposed extension presents the advantage of providing reasonable estimates of the nonlinear steady-state characteristics.

Keywords: Control valves; Nonlinear models; Identification algorithms; Friction.

1. INTRODUCTION

Friction in control valves and inadequate controller tuning are two of the major sources of control loop performance degradation (Jelali, 2006). While process models play an essential role in controller design, friction models are needed to diagnose abnormal valve operation or to compensate such undesirable effects. Hence, methods for valve friction quantification and process models identification arise as important tools to treat loop performance problems.

For practical reasons, it is desirable that such methods should be based only on controller output (*op*) and process output (*pv*) measurements from closed-loop experiments. Choudhury et al. (2004) dealt with friction quantification by fitting an ellipse to *pv-op* data, but the results produced by this technique depend on the controller tuning. Häggglund (2007) approximated the nonlinear valve behavior with a backlash structure, which is estimated using the process static gain and the controller tuning parameters.

In a method proposed by Srinivasan et al. (2005), an optimization approach is used to jointly estimate the process dynamics and the friction model parameters. This method can be seen as a Hammerstein model identification, since the valve friction is treated as a nonlinear block followed by a linear dynamic block that represents the process. As the process dynamics is also estimated, the joint procedure previously mentioned can be used for controller retuning. However, in that work, an inappropriate friction model structure that is unable to reproduce important sticky valve characteristics is employed. Choudhury et al. (2008) eliminated this drawback adopting a two-parameter friction model structure.

Another extension to the method originally conceived by Srinivasan et al. (2005) was recently proposed (Romano and Garcia, 2009) so that a Wiener model (built up with a linear dynamic block \mathcal{L} connected to a nonlinear static function \mathcal{N}_2) was considered to represent the process. In this approach the Hammerstein structure is extended to a Hammerstein-Wiener one (Figure 1), i.e., the valve friction is associated with the first nonlinear block (\mathcal{N}_1), while the remainder blocks represent the process.

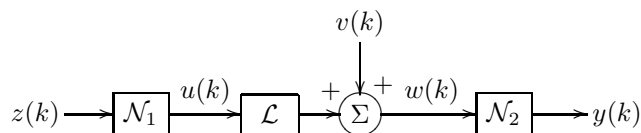


Fig. 1. Hammerstein-Wiener model structure with nonlinear disturbance.

Despite providing some features (e.g., to avoid that process nonlinearities be erroneously incorporated in the friction model and to turn the estimation method suitable to wider operating ranges), the previous proposal demands considerably computation effort, since the friction model parameters are estimated through direct search. In this work, the method proposed by Romano and Garcia (2009) is improved, so that optimization is applied in the friction quantification. In addition, the new extension is tested in a HIL (hardware-in-the-loop) setup, in which the influences of the signal-noise ratio, as well as of the controller tuning are investigated in a more realistic framework.

The paper is organized as follows: the friction model is described in Section 2. The parameterization of the process model, as well as an estimation algorithm are presented in Section 3. The friction and process model joint estimation procedure based on optimization is treated in Section 4.

The HIL platform results are discussed in Section 5. At last, the conclusions are drawn.

2. VALVE FRICTION MODEL

Several friction models were evaluated using ISA standard tests in Garcia (2008). The best trade-off between accuracy and simplicity was achieved by the data-driven two-parameter model proposed by Kano et al. (2004). The parameter S represents the cumulative input signal $z(k)$ amplitude change necessary to revert the valve movement direction, while J is the size of the stem slip observed when the valve starts to move, also referred as *slip-jump*.

Besides the parameters S and J , the friction model uses three auxiliary variables: stp that indicates if the valve is moving ($stp = 0$) or if it is stuck ($stp = 1$), z_s that is updated with $z(k)$ every time the valve sticks and $d = \pm 1$ that denotes the direction of the friction force.

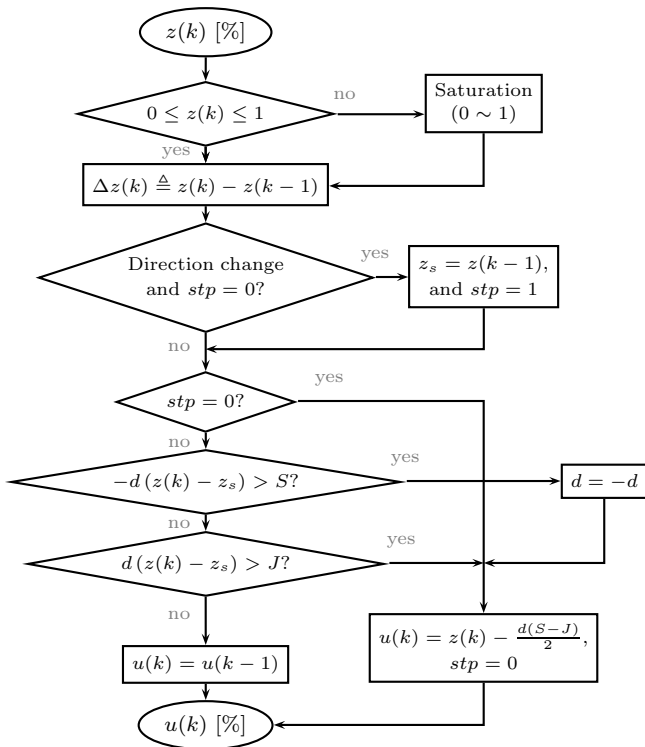


Fig. 2. Flowchart of the data-driven model parameterized by S and J (Kano et al., 2004).

The relationship between the command signal $z(k)$ and the valve stem position $u(k)$ is described in the flowchart shown in Figure 2. After testing whether the valve stopped, so that z_s and stp are eventually updated, a new value is assigned to $u(k)$ if: (i) the valve is moving ($stp = 0$), (ii) the valve changes its direction and overcomes S or (iii) the valve moves in the same direction and overcomes J . On the contrary, the position remains the same.

3. WIENER MODEL IDENTIFICATION

3.1 Process model parameterization

As argued earlier the association $\mathcal{L} \rightarrow \mathcal{N}_2$ depicted in Figure 1 is a Wiener model that represents the process

dynamics. Thus, $v(k), u(k)$ and $y(k)$ denote the process disturbances, input and output signals, respectively.

The linear block \mathcal{L} is represented by an ARMAX model:

$$w(k) = G(q)u(k) + H(q)e(k) \quad (1)$$

where q is the shift operator: $q^{-i}y(k) = y(k-i)$, $e(k)$ is white noise with zero mean and variance σ_e^2 , $G(q)$ and $H(q)$ are rational transfer functions parameterized by l and n_c :

$$G(q) = \frac{B(q)}{A(q)} = \frac{b_1q^{-1} + \dots + b_lq^{-l}}{1 + a_1q^{-1} + \dots + a_lq^{-l}} \quad (2)$$

$$H(q) = \frac{C(q)}{A(q)} = \frac{1 + c_1q^{-1} + \dots + c_{n_c}q^{-n_c}}{1 + a_1q^{-1} + \dots + a_lq^{-l}} \quad (3)$$

Cubic splines provide advantages in respect of polynomials and piecewise linear functions to approximate arbitrary nonlinear functions (Lancaster and Šalkauskas, 1986). For a set of m different knots:

$$w_{\min} = w_1 < w_2 < \dots < w_{m-1} < w_m = w_{\max} \quad (4)$$

A cubic spline can be expressed by:

$$\begin{aligned} y(k) &= f(w(k)) \\ &= \sum_{i=2}^{m-1} f_i |w(k) - w_i|^3 + f_m + f_{m+1}w(k) \end{aligned} \quad (5)$$

where $\eta \triangleq (f_2, \dots, f_{m+1})^T$ is the cubic spline parameter vector and $w(k)$ is the signal between \mathcal{L} and \mathcal{N}_2 .

3.2 Wiener model parameter estimation

In this work, two assumptions are made in order to estimate the Wiener model parameters in (1) and (5): (i) the function $f(\cdot)$ which describes the process nonlinearity is monotonic and invertible and (ii) the process is open-loop stable. It should be stressed that both assumptions are commonly found in many practical situations, e.g., CSTRs and distillation columns.

Due to the first assumption, analogously to (5), the inverse of the process nonlinearity $f^{-1}(\cdot)$ is denoted by:

$$w(k) = \sum_{i=2}^{m-1} g_i |y(k) - y_i|^3 + g_m + g_{m+1}y(k) \quad (6)$$

Thus, the Wiener model parameters are obtained from the minimization of the following criterion (Zhu, 2001):

$$V = \sum_k (H^{-1}(q) (f^{-1}(y(k)) - G(q)u(k)))^2 \quad (7)$$

Since (7) is highly nonlinear, instead of minimizing V directly, an overparameterized model is estimated. Afterwards, a model reduction is performed to achieve the ARMAX model described in (1).

Under the assumption that the process is open-loop stable, it is possible to approximate the dynamic block \mathcal{L} by a finite impulse response (FIR) model, so that the intermediate signal is expressed by:

$$w(k) = \beta_1 u(k-1) + \dots + \beta_n u(k-n) + v(k) \quad (8)$$

For a more compact notation, consider the regression $\psi(k)$ and the parameter θ vectors:

$$\psi(k) \triangleq \left(-|y(k) - y_2|^3, \dots, -|y(k) - y_{m-1}|^3, -1, \right. \\ \left. u(k-1), \dots, u(k-n) \right)^T \quad (9)$$

$$\theta \triangleq (g_2, \dots, g_{m-1}, g_m, \beta_1, \dots, \beta_n)^T \quad (10)$$

Considering (7)-(10), θ can be estimated minimizing the disturbance term $v(k)$:

$$\hat{\theta} = \arg \min_{\theta} \sum_k (\psi^T(k) \cdot \theta)^2 \quad (11)$$

However, as the intermediate signal $w(k)$ is unmeasurable, the gain of the Wiener model can be arbitrarily distributed between the dynamic and the static block. To avoid the trivial solution $\theta = 0$, the following constraint is imposed on (11):

$$\sum_{i=1}^n \beta_i = 1 \Rightarrow \underbrace{(0 \dots 0)}_m \underbrace{(1 \dots 1)}_n \cdot \theta = \mathcal{R} \cdot \theta = 1 \quad (12)$$

Since this constraint is linear, the solution of (11) subject to $\mathcal{R} \cdot \theta = 1$ is given by (Pearson and Pottmann, 2000):

$$\hat{\theta} = (\Psi^T \Psi)^{-1} \mathcal{R}^T \left(\mathcal{R} (\Psi^T \Psi)^{-1} \mathcal{R}^T \right)^{-1} \quad (13)$$

where $\Psi \triangleq (\psi(n+1) \dots \psi(N))^T$ and N is the length of the estimation dataset.

To obtain $G(q)$ and $H(q)$ defined in (1), a model reduction is accomplished by minimizing the criterion V_{red} :

$$V_{red} = \sum_k \left(H^{-1}(q) \left(\sum_{i=1}^n \hat{\beta}_i u(k-i) - G(q)u(k) \right) \right)^2 \quad (14)$$

which can be seen as the ARMAX model estimate using the prediction error method (Zhu, 2001), considering the intermediate signal calculated with the FIR model (8).

Finally, the nonlinear block parameter vector η estimate is given by:

$$\hat{\eta} = \arg \min_{\eta} \sum_k (y(k) - \phi^T(k) \cdot \eta)^2 \quad (15)$$

where:

$$\phi(k) \triangleq \left(|\hat{w}(k) - w_2|^3, \dots, |\hat{w}(k) - w_{m-1}|^3, 1, \hat{w}(k) \right)^T \\ \hat{w}(k) \triangleq \hat{f}^{-1}(y(k))$$

Due to the approximation of the linear dynamic block by a FIR structure, an initial estimate is computed analytically from (13), at the expense of increasing the amount of parameters, and consequently, the variance of the estimate. After that, the FIR model is reduced to diminish the variance of the estimate and to achieve a model structure suitable for control applications.

The model orders l , n_c and m can be selected by trial and error or based on the simulation error (Zhu, 2001).

4. FRICTION AND PROCESS MODEL JOINT IDENTIFICATION ALGORITHM

Figure 3 denotes a control loop in the presence of valve friction. The problem to be treated is to quantify the friction and estimate a nonlinear process model by means of controller output $z(k)$ and process output $y(k)$. Moreover, a test signal $d(k)$ can be introduced into the set-point $r(k)$ to improve the data signal-noise ratio (SNR).

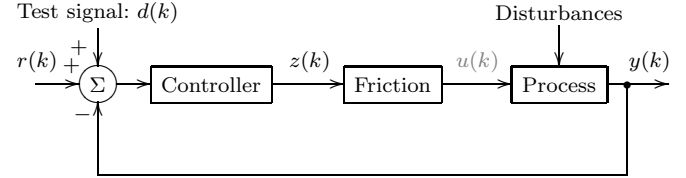


Fig. 3. Process control loop subject to valve friction.

The valve friction model parameterized by the pair (S, J) connected to a Wiener model denoting the process is shown in Figure 4.

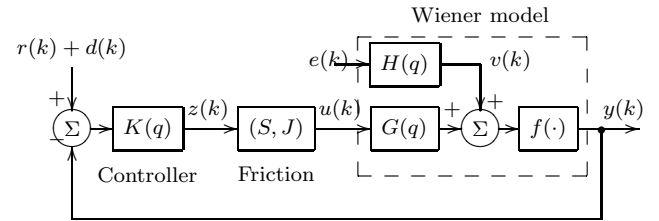


Fig. 4. Control loop where the valve friction and the process are modeled by a Hammerstein-Wiener structure.

For fixed values of the pair (S, J) it is possible to calculate the input $u(k)$ using the nonlinear transformation $\mathcal{F}(\cdot)$ which is described in the flowchart of Figure 2, i.e.:

$$\hat{u}(k, S, J) = \mathcal{F}(z(k), z(k-1), \hat{u}(k-1), S, J) \quad (16)$$

Hence, the Wiener model parameters can be estimated, with (16) and the measured output $y(k)$. However, the pair (S, J) is unknown. In this work, instead of testing all combinations in a set of candidate values, the Nelder-Mead Simplex algorithm (Lagarias et al., 1998) is considered for searching the optimal pair. This gradient-free optimization method is suitable to minimizing discontinuous functions such as the friction nonlinearity.

The Simplex algorithm initialization is a key issue in the parameter estimation procedure, because a “good” initial guess not only increases the probability of finding the global optimum but also speeds up the convergence. The initial guess (S_0, J_0) is calculated disconsidering J and performing a grid search over S with step size ΔS . The procedure for estimating the friction and the nonlinear process model parameters is summarized as follows:

Algorithm 1. Friction and nonlinear process model identification using optimization for searching S and J .

- i. Generate a set \mathcal{D}_S of candidate values for S :

$$\mathcal{D}_S = \left(0, \Delta S, 2\Delta S, \dots, S_{max} \right) \quad (17)$$

- ii. Supposing $J = 0$, for each value $S_i \in \mathcal{D}_S$, calculate $\hat{u}(k, S_i)$ from (16). Then, estimate the process model parameters $\hat{G}(q)$ and $\hat{f}(\cdot)$;

iii. Compute the simulation error C_i :

$$C_i = \sum_k \left(y(k) - \hat{f} \left(\hat{G}(q) \hat{u}(k, S_i) \right) \right)^2 \quad (18)$$

iv. Select S° among the candidate values S_i that minimize C_i and compute the initial condition:

$$(S_0, J_0) = (S^\circ + \gamma \Delta S, \gamma \Delta S) \quad (19)$$

v. From the initial guess (S_0, J_0) , solve the optimization problem with the Simplex algorithm:

$$(S^*, J^*) = \arg \min_{(S, J)} \sum_k (y(k) - \hat{y}(k))^2 \quad (20)$$

where: $\hat{y}(k) = \hat{f} \left(\hat{G}(q) \hat{u}(k, S, J) \right)$;

vi. Estimate the Wiener model parameters with $y(k)$ and $\hat{u}(k, S^*, J^*)$.

Remark: The initial condition (19) is motivated by the stem position update equation (Figure 2):

$$u(k) = z(k) - \frac{d}{2}(S - J) \quad (21)$$

Assuming $J = 0$ implies $S^\circ \pm \Delta S \approx S - J$. Hence, initializing J as a multiple of ΔS results in (19). Furthermore, as bench tests have suggested that the backlash in control valves is greater than the *slip-jump* (Romano and Garcia, 2008), it is convenient to evaluate the fit between y and \hat{y} with increasing values of γ . The parameters that provide the best fit are chosen.

5. EXPERIMENTS AND RESULTS

The friction and process model parameters estimation algorithm is tested in a HIL setup, where a real valve (model *ET, Fisher Inc.*) is integrated with a pH neutralization process simulated in real-time. A simplified diagram of the system is depicted in Figure 5. The process consists of three input flows: acid q_1 , buffer q_2 and base q_3 that are mixed in tank T1. The controlled variable is the pH in T1. The manipulated variable is the base flow, which is controlled by the real valve (AV) stem position that is measured with a LVDT sensor. The alkaline solution is stored in a pressurized tank T2. In addition, a level loop maintains the T1 level manipulating the outflow q_4 by means of the valve LV, that is simulated without friction. The neutralization process model equations, as well as the nominal operating conditions are presented in appendix A.

During the experiment, the acid and the base concentrations, as well as the acid flow are disturbed by independent white noise realizations filtered by discrete transfer functions with pole: 0.9, 0.85 and 0.8, respectively. To give an idea of the disturbance magnitude, the acid and the base concentrations oscillated up to 2.15% and 10.65% around the nominal value, while q_1 varied up to 3.75%.

The pH loop PI controller (AIC) is tuned with the Direct Synthesis method (Bequette, 2003). Firstly, the AIC parameters are computed so that the closed-loop dominant time constant τ_{cl} is 80% of the open-loop one τ_{ol} , which was previously estimated using step tests around the nominal operating conditions ($\tau_{ol} = 42s$). The test signal $d(k)$ is a binary random noise with average switching time of 20 samples (80s). To analyze the test signal magnitude

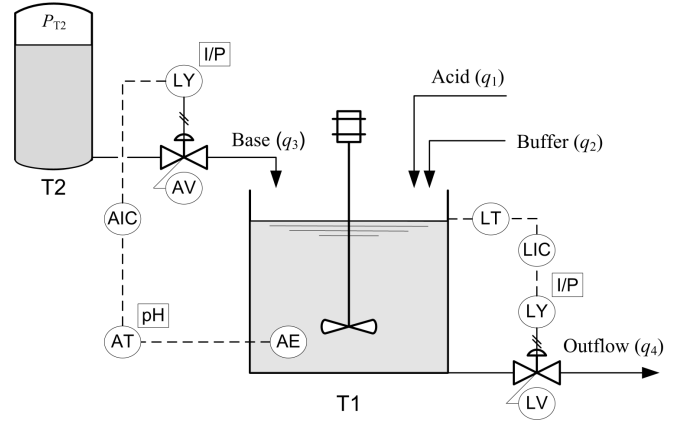


Fig. 5. The pH neutralization process diagram.

influence, four experiments are performed using increasing magnitudes, while $r(k)$ is maintained constant in 7.

The model fit to experimental data is quantified by \mathcal{F}_2 :

$$\mathcal{F}_2[\%] = \left(1 - \frac{\|\hat{Y} - Y\|_2}{\|Y - \bar{Y}\|_2} \right) \times 100 \quad (22)$$

where Y , \bar{Y} and \hat{Y} are the experimental output vector, the output mean and the estimated output, respectively. In this work, the output vector is composed of data from a distinct experiment without disturbances. The static curve fit is quantified using a linear correlation coefficient:

$$r_N[\%] = \frac{\text{cov}(Y^0, \hat{Y})}{\text{std}(Y^0) \cdot \text{std}(\hat{Y})} \times 100 \quad (23)$$

Once the titration curve is known, it is employed to calculate the true steady-state Y^0 with a set of intermediate variable $w(k)$ values. The symbol $\text{std}(\cdot)$ indicates standard deviation and $\text{cov}(\cdot, \cdot)$ denotes covariance.

A 1000 samples dataset is used for estimation purposes. Moreover, the algorithm parameterizations are:

$$\Delta S = 0.02, n = 45, l_{max} = 4, m_{max} = 9 \text{ and } n_c = 2.$$

All the combinations of (l, m) from $(1, 3)$ to (l_{max}, m_{max}) were tested, but only the model order that provided the best \mathcal{F}_2 was selected. The results for increasing magnitude test signals are summarized in Table 1, which reveals that the estimate of the pair (S, J) in each situation is similar.

Table 1. Synthesis of the results achieved for increasing $d(k)$ magnitudes.

Magnitude of $d(k)$	S [%]	J [%]	\mathcal{F}_2 [%]	r_N [%]
0% pH_{nom}	25.35	2.17	40.85	97.5791
$\pm 2.5\%$ pH_{nom}	24.38	2.21	59.33	99.2826
$\pm 5\%$ pH_{nom}	25.05	2.03	82.22	99.9852
$\pm 10\%$ pH_{nom}	25.35	2.18	85.62	99.1942

On the other hand, \mathcal{F}_2 indicates that the process model quality degrades for a test signal switching between $\pm 2.5\%$ pH_{nom} or when $d(k) = 0$ (natural excitation). There are two reasons for such fact: (i) the data SNR is proportional to the magnitude of $d(k)$ and (ii) due to the friction, smaller variations in $z(k)$ can be insufficient to change the manipulated variable $u(k)$ that implies less informative experiments.

Another aspect relative to Table 1 is that the higher magnitude ($\pm 10\% \text{pH}_{nom}$) excitation yields a r_N that is not the closest to 1. It occurs because the computation of r_N considers only the range where the process is tested. Hence, experiments restricted to a narrower range can, eventually, report a better linear correlation coefficient, despite of not reproducing the steady-state behavior so accurately in a wider range. This is confirmed in Figure 6. In fact, higher data SNR implies more steady-state estimation accuracy in wider ranges.

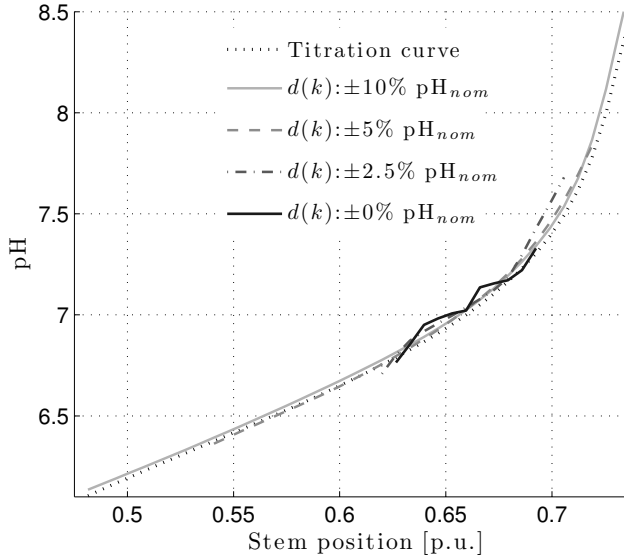


Fig. 6. Titration and estimated steady-state curves.

Some friction quantification techniques (Choudhury et al., 2004; Hägglund, 2007) are influenced by the loop controller gain. In order to investigate this issue, the AIC controller is retuned using other three specifications: one more conservative and two more aggressive than $\tau_{cl} = 0.8\tau_{ol}$. The experiments are performed with a $d(k)$ magnitude of $\pm 5\% \text{pH}_{nom}$.

The results presented in Table 2 indicate that the friction and the process model parameters estimate are not significantly affected by different controller tuning. Nevertheless, the more aggressive tuning yielded the worst \mathcal{F}_2 , that quantifies the overall fit. The estimate of the steady-state curve is also the worst in this situation as can be seen in Figure 7. This is justified by the process oscillatory behavior caused by the high controller gain which leads to a dataset with few static characteristic information.

Furthermore, it should be highlighted that the misfit of the steady-state curve for $\text{pH} > 8$ exhibited in all situations is due to the substantial variation of the static behavior associated with the reduced amount of samples in this operating range.

With the purpose of validating the friction model parameters, the measured stem position from an open-loop exper-

Table 2. Results with different controller gains.

Specification	S [%]	J [%]	\mathcal{F}_2 [%]	r_N [%]
$\tau_{cl} = \tau_{ol}$	25.48	2.20	81.17	99.9108
$\tau_{cl} = 0.8\tau_{ol}$	25.05	2.03	82.22	99.9852
$\tau_{cl} = 0.5\tau_{ol}$	26.19	2.12	87.90	99.6816
$\tau_{cl} = 0.2\tau_{ol}$	23.59	1.83	72.23	99.8725

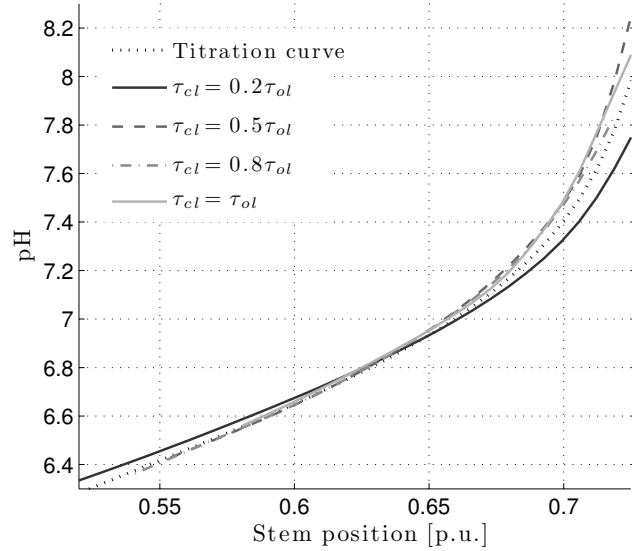


Fig. 7. Steady-state behavior of models estimated with different controller.

iment excited with a multilevel signal is compared to the simulated one. Since the (S, J) values reported in Tables 1 and 2 are similar, only the stem position calculated using the friction model parameter estimate averages is compared to the actual one (LVDT measurement). Note from Figure 8 that the friction model output accurately tracks the actual stem position. It demonstrates that the two-parameter model with the estimated pair (S, J) is able to reproduce the real valve friction behavior.

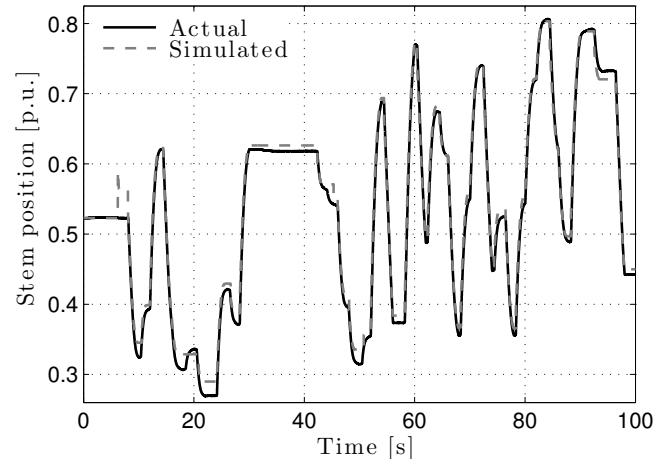


Fig. 8. Simulated and actual valve stem position.

6. CONCLUSIONS

The results provided by the HIL setup indicates that, despite of the controller tuning, the proposed estimation algorithm is not only able to quantify the friction but also can identify a nonlinear process model since a test signal is employed to guarantee the loop excitation. Nevertheless, even without an external excitation signal, it is possible to find reliable values for S and J .

Differently from other methods (Srinivasan et al., 2005; Choudhury et al., 2008; Jelali, 2008) solely based on normal operating data, in this work, the friction quantification

and the process model identification are equally important. However, even if the aim is restricted to quantifying the valve friction, obtaining a suitable process model is vital to validate the friction model through simulations. The results reported that signals with higher amplitude provided better models, while the natural excitation experiment yielded inaccurate ones. Therefore, the adoption of a test signal should be considered whenever possible, in order to improve the process model estimate.

Another contribution of this work is the friction model parameters search using the Simplex algorithm from an initial guess calculated disregarding J . As a consequence the computational effort is drastically reduced compared to exhaustive search. Alternatively, pattern search could also be used to estimate S and J as in Jelali (2008).

REFERENCES

- Bequette, B.W. (2003). *Process Dynamics: Modeling, Analysis, and Simulation*. Prentice Hall, Upper Saddle River, NJ.
- Choudhury, M.A.A.S., Jain, M., Shah, S.L., and Shook, D.S. (2008). Stiction - definition, modelling, detection and quantification. *Journal of Process Control*, 18, 232–243.
- Choudhury, M.A.A.S., Shah, S.L., and Thornhill, N.F. (2004). Detection and quantification of control valve stiction. In *Proceedings of the 7th IFAC Symposium on dynamics and control of process systems (DYCOPS)*. Cambridge, MA, USA.
- Garcia, C. (2008). Comparison of friction models applied to a control valve. *Control Engineering Practice*, 16(10), 1231–1243.
- Hägglund, T. (2007). Automatic on-line estimation of backlash in control loops. *Journal of Process Control*, 17, 489–499.
- Henson, M.A. and Seborg, D.E. (1997). Adaptive input-output linearization of a pH neutralization process. *International Journal of Adaptive Control and Signal Processing*, 11, 171–200.
- Jelali, M. (2006). An overview of control performance assessment technology and industrial applications. *Control Engineering Practice*, 14, 441–466.
- Jelali, M. (2008). Estimation of valve stiction in control loops using separable least-squares and global search algorithms. *Journal of Process Control*, 18, 632–642.
- Kano, M., Hiroshi, M., Kugemoto, H., and Shimizu, K. (2004). Practical model and detection algorithm for valve stiction. In *Proceedings of the 7th IFAC Symposium on dynamics and control of process systems (DYCOPS)*. Cambridge, MA, USA.
- Lagarias, J.C., Reeds, J.A., Wright, M.H., and Wright, P.E. (1998). Convergence properties of the Nelder-Mead Simplex method in low dimensions. *SIAM Journal on Optimization*, 9(1), 112–147.
- Lancaster, P. and Šalkauskas, K. (1986). *Curve and Surface Fitting: An introduction*. Academic Press, London.
- Pearson, R.K. and Pottmann, M. (2000). Gray-box identification of block-oriented nonlinear models. *Journal of Process Control*, 10, 301–315.
- Romano, R.A. and Garcia, C. (2008). Karnopp friction model identification for a real control valve. In *Proceedings of the 17th IFAC World Congress*. Seoul, Korea.
- Romano, R.A. and Garcia, C. (2009). Valve friction and nonlinear process model closed-loop identification. In *Proceedings of the 7th IFAC International Symposium on Advanced Control of Chemical Processes (AD-CHEM)*.
- Srinivasan, R., Rengaswamy, R., Narasimhan, S., and Miller, R. (2005). Control loop performance assessment. 2. Hammerstein model approach for stiction diagnosis. *Industrial & Engineering Chemistry Research*, 44(17), 6719–6728.
- Zhu, Y. (2001). *Multivariable System Identification for Process Control*. Elsevier Science, Oxford.

Appendix A. NEUTRALIZATION PROCESS MODEL

The pH neutralization process is simulated by the following equations:

$$\dot{h}_{T2}(t) = -\frac{1}{A_{T2}}q_3(t) \quad (A.1)$$

$$q_3(t) = K_{q3} \cdot X_{AV}(t) \sqrt{P_{T2} + \rho \cdot g \cdot h_{T2}(t)} \quad (A.2)$$

$$\dot{h}_{T1}(t) = \frac{1}{A_{T1}}(q_1(t) + q_2(t) + q_3(t) - q_4(t)) \quad (A.3)$$

$$q_4(t) = K_{q4} \cdot X_{LV}(t) \sqrt{\rho \cdot g \cdot h_{T1}(t)} \quad (A.4)$$

$$X_{LV}(t) = K_{c(LIC)} \left(e_{hT1} + \frac{1}{T_{i(LIC)}} \int_{t_0}^t e_{hT1} d\tau \right) \quad (A.5)$$

$$e_{hT1} = h_{T1}(t) - h_{T1nom} \quad (A.6)$$

$$\dot{W}_{a4}(t) = \frac{1}{A_{T1}h_{T1}(t)} \sum_{i=1}^3 q_i(t) (W_{a_i} - W_{a4}(t)) \quad (A.7)$$

$$\dot{W}_{b4}(t) = \frac{1}{A_{T1}h_{T1}(t)} \sum_{i=1}^3 q_i(t) (W_{b_i} - W_{b4}(t)) \quad (A.8)$$

The model is based on the reaction invariant theory from which the pH is given by a nonlinear function of W_{a4} and W_{b4} . For more details refer to (Henson and Seborg, 1997). The nominal operating conditions are shown in Table A.1.

Table A.1. Nominal operating conditions.

Description	Symbol	Value
Tank T1 area	A_{T1}	0, 1 m ²
Initial condition of (A.3)	h_{T1nom}	0, 1 m
Tank T2 area	A_{T2}	0, 5498 m ²
Initial condition of (A.1)	h_{T2max}	1 m
T2 nominal pressure	P_{T2}	$1, 2 \times 10^6 \frac{N}{m^2}$
Solution specific mass	ρ	$1000 \frac{kg}{m^3}$
Gravitational acceleration	g	$9, 80665 \frac{m}{s^2}$
Hydraulic constant of AV	K_{q3}	$1, 5189 \times 10^{-7} \frac{m^4}{s\sqrt{N}}$
Hydraulic constant of LV	K_{q4}	$1, 5226 \times 10^{-5} \frac{m^4}{s\sqrt{N}}$
AV nominal stem position	X_{AVnom}	0, 6584 p.u.
LV nominal stem position	X_{LVnom}	0, 5 p.u.
Nominal acid flow	q_{1nom}	$1, 22 \times 10^{-4} \frac{m^3}{s}$
Nominal buffer flow	q_{2nom}	$6, 4 \times 10^{-6} \frac{m^3}{s}$
Nominal base flow	q_{3nom}	$1, 1 \times 10^{-4} \frac{m^3}{s}$
pH nominal value	pH_{nom}	7
LIC controller gain	$K_{c(LIC)}$	0, 1777
LIC integral time	$T_{i(LIC)}$	26, 5 s/rep